# Seismic demands of steel buildings with perimeter and spatial moment resisting frames

**A. Reyes-Salazar[1],\*, E. Bojorquez[1], J.L. Rivera-Salas[1], A. Lopez-Barraza[1], H.E. Rodriguez-lozoya[1]**

## Abstract

The linear and nonlinear responses of steel buildings with perimeter moment resisting frames (PMRFs) are estimated and compared to those of equivalent buildings with spatial moment resisting frames (SMRFs). The equivalent models with SMRFs are designed by using an approximated procedure in such a way that, not only their fundamental period, total mass and lateral stiffness are fairly the same as those of the corresponding buildings with PMRFs, but also other characteristics to make the two structural "as equivalent" as possible. The numerical study indicates that the interstory shears of the PMRFs building may be significantly larger than those of the SMRFs building. The main reasons for this are that the buildings with PMRFs are stiffer and that the dynamics properties of the two types of structural systems are different. The interstory displacements are similar for both structural systems in many cases. For some other cases, however, they are larger for the model with SMRFs, depending upon the closeness between the earthquake corner periods and the periods of the buildings. The global ductility and story ductility demands are larger for the buildings with PMRFs, implying that, since larger ductility demands are imposed, the detailing of the connections will have to be more stringent than for the buildings with SMRFs. It can be concluded, that the seismic performance of the steel buildings with SMRFs may be superior to that of steel buildings with PMRFs. The findings of this paper are for the particular models used in the study. Much more research is needed to reach more general conclusions.

## 1. Introduction

Among the different structural systems used to support lateral seismic loading, moment resisting steel frames (MRSFs) are broadly used for the case of steel buildings. They have been popular systems because they provide maximum flexibility for space utilization and because of their high ductility capacity. The basic structural arrangement of this structural system, however, has significantly changed over the years. From the mid 60s to the mid 70s, at least in USA, most of the connections in steel buildings were fully restrained connections (FRCs), resulting in highly redundant buildings. For the case of weak axis connection, it was the standard practice for many years [1] to frame the beams to the columns by welding the beam flange to a continuity plate which in turn was welded to the web and the flanges of the column.

Tests have shown [2] that this type of weak-axis connection is susceptible to fracture at the weld connecting the beam flange to the continuity plate.

However, this problem can be mitigated by using several measures, including extending the continuity plate beyond the column flanges. Because the mitigation procedure is expensive, the standard practice during the recent past (after the 80s) has been to eliminate weak-axis moment connections. Most of the steel buildings with MRSFs built in USA have FRCs only on two frame lines in each direction, usually at the perimeter, and often these frames do not extend over the full plan of the buildings. These frames are used to support the total seismic lateral load while Gravity Frames (GFs), used at the interior, are used to support the gravity loads. In these frames, the beam-to-column connections are assumed to be perfectly pinned (PP). Several steel buildings suffered brittle failures in their welded connections (major-axis) during the Northridge Earthquake of 1994. Thus the undesirable brittle behavior may occur, not only for FRCs with respect to the minor axis, but also with respect to the major axes. FEMA [1] suggested structural arrangements and member sizes of some such model buildings to study their behavior and investigate the causes of failures.

The main advantages of using steel buildings with perimeter MRSFs are that they are considered to behave in two dimensions within a three-dimensional structure providing a simpler frame to analyze and design and that using fewer MRCs introduces overall economy in the design since these connections are expensive. However,

\* Corresponding author: reyes@uas.edu.mx

1 Universidad Autónoma de Sinaloa, Facultad de Ingeniería, Universidad Autónoma de Sinaloa, Calzada de las Américas y Blvd. Universitarios S/N, Ciudad Universitaria, Culiacán, Sinaloa, México, CP 80040

there are several disadvantages too, some of them are: (a) since the size the girders of MRSFs is very large, the amount of strain demand placed on the welded connection elements is also too large, making the connections more susceptible to brittle behavior [1]; (b) the perimeter MRSFs, modeled as plane frames, are usually designed to resist the total lateral seismic loading, ignoring the contribution of the GFs. Due to the action of rigid floor diaphragms the columns of these GFs, however, will bent undergoing a similar lateral deformation than the MRSFs, consequently, their contribution of these columns to the lateral resistance could be significant which is totally ignored [3]; and (c) because much fewer FRCs are used in comparison with spatial moment resisting connections, the redundancy of the building is tremendously reduced. The relatively low redundancy of steel buildings with perimeter MRSFs has been appointed by the engineering community as one of the possible causes of their poor seismic performance [4]. In section 2.5.4 of FEMA 350 [5] it is stated "there are several reasons why structures with some redundancy in their structural systems should perform better than structures without such redundancy. Redundant structures, on the other hand, would still retain some significant amount of lateral resistance following failure of a few elements."

In Mexico, it is common to use steel buildings with MRSFs at the perimeter and the interior [6] in both horizontal directions. Due to the large number of FRCs of this system, its redundancy and ductility capacity are expected to be greater than those of the systems with only perimeter MRSFs, although the structural analysis is more complicated. Comparison of the performance of these two structural systems under the action of severe seismic loads is undoubtedly of great interest to the profession and therefore it is addressed in this research.

Significant research has been developed regarding the seismic behavior of buildings with MRSFs. Lee and Foutch [7] studied the seismic behavior of 26 post-Northridge buildings that represent typical steel MRSFs buildings, subjected to sets of 20 SAC ground motions representing the 2/50 and 50/50 hazard levels. They concluded that all of the post-Northridge buildings exhibit a high confidence of performing. Foutch and Yun [8] investigated the accuracy of simple nonlinear as well as more detailed modeling methods used in the design of MRSFs. They showed that the model which incorporates clear length dimensions between beams and columns, panel zones and an equivalent gravity bay without composite action from the slab could be a practical model with good accuracy. Gupta and Krawinkler [9] studied the behavior of various models designed according to the design provisions of various U.S. cities. Mele and Others [4] compared the seismic behavior of steel buildings with perimeter MRSFs with the corresponding responses of steel buildings with perimeter and some interior FRCs in the strong direction, finding that the response of both systems is similar in terms of local and global response parameters

In another study, Lee and Foutch [10] studied the seismic behavior of 3-, 9-, and 20-story MRSFs designed

for different reductions (R) factors. A total of 30 different structural models and 20 ground motions were used. The results showed that the current R factors provide conservative designs for low-rise steel buildings but showed a low level of confidence for high buildings. Krishnan et al [11] determined the damage produced by hypothetical earthquakes on two 18-storey MRSFs, one existing and one improved according to the 1997 Uniform Building Code [12], located in southern California, USA. They concluded that severe damage could occur in these buildings. The redesigned building performed significantly better than the existing one, however, the design based on the 1997 UBC was still not adequate to prevent serious damage. Kazantzy et al [13] proposed a methodology for the probabilistic assessment of low-rise steel buildings and applied it to a welded MRSF, emphasizing the modeling of connections. They found that structures experiencing brittle connection fractures undergo large deformations, resulting in a low reliability in terms of achieving code-related performance parameters. Liao et al [14] developed a three-dimensional finite-element model to examine the effects of bi-axial motion and torsion on the nonlinear response of MRSFs. Effects of gravity frames, panel zones, and inelastic column deformation are also considered. Results indicated that torsional effects due to asymmetric member failures are important, that the conventional lumped-plasticity model limits the plasticity of columns and that fracture failures of the pre-Northridge connections have a severe impact on the buildings performance. More recently, Chang et al [15], by using 6- and -20 level steel office buildings, studied the role of accidental torsion in seismic reliability assessment. They concluded that ignoring the accidental torsion can lead to an unsafe evaluation for the strength of the building fragilities and that, on the other hand, the use of code accidental eccentricity may give conservative estimates.

The seismic nonlinear response of steel plane frames with MRSFs considering the dissipation of energy has been also studied [3, 16, 17, 18, 19, and 20]. These studies showed that the dissipation of energy has an important effect on the structural response.

In spite of the amount of research developed in the area of seismic behavior of steel buildings with MRSFs and the important contributions of the earlier-mentioned and other studies, the comparison of the performance of three-dimensional steel buildings with perimeter and spatial MRSFs in terms of redundancy and ductility have not been studied. Moreover, the plastic energy developed in the structural elements, which is related to the damage in them, has not been explicitly considered. The seismic responses of these two structural systems are expected to be different since they dynamic characteristics are different too. The estimation and comparison of the linear and nonlinear seismic responses of these structural systems constitute the main objective of the present investigation.

To meet the objectives of the study, the behavior of some steel buildings with perimeter and spatial MRSFs, needs to be represented as realistically as possible, preferably in 3-D and then estimating responses by exciting them with measured seismic time histories. Specifically, the linear and

nonlinear seismic responses, in terms of interstory shears, interstory displacements, ductility and plastic energy, are estimated for steel buildings with perimeter MRSFs and compared with those of their equivalent steel buildings with spatial MRSFs. The models are analyzed in the time domain under the action of 20 recorded earthquakes. They are obtained from the Data Sets of the National Strong Motion Program (NSMP) of the United States Geological Surveys (USGS) and were selected to represent the characteristics of strong motion earthquakes. The study will provide some design guidelines to be considered by the profession regarding the seismic behavior of steel buildings with perimeter and spatial MRSFs.

## 2. Ductility Definitions

The ductility parameter plays an important role in the determination of the design seismic forces. It is related to the capacity of a structure to dissipate energy. It is particularly important for steel structures since the beneficial effect of ductility is supposed to come from different sources. Although the concept of ductility is constantly used by the profession, at present there is no engineering definition of it in the specifications and codes and there is no unanimity in the profession on how to define it. It is used in an indirect way in design. In a research report [21] it was stated, "Ductility is shown in parentheses to emphasize that there is no definition of ductility in our Specification and Codes but it is always being used. The metallurgical definition of ductility is the ability of a metal to be stressed beyond its yield strength and into its plastic (inelastic) range, with large elongations before rupturing in a ductile mode. An engineering definition of ductility may be needed, as related to moment-resisting frames design and construction."

As stated earlier, the seismic responses of the two structural systems under consideration are also studied in terms of ductility demands. A definition of ductility is adopted here for that purpose.

### 2.1. Ductility definitions

In the context of seismic analysis of single degree of freedom (SDOF) systems, ductility can be conceptually defined as the ratio of the maximum inelastic displacement ($D_{max}$) to the yield displacement ($D_y$). $D_y$ can be defined as the displacement of the system when it yields for the first time and $D_{max}$ as the maximum displacement that the system undergoes during the application of the complete earthquake loading. For MDOF systems there is no unanimity in the profession on how to define it. Definition of story and global ductility proposed by Reyes-Salazar [22] and used in other investigations [23] are adopted in this study.

### 2.1.1. Story ductility (μ)

For each story, $D_{max}$ is the maximum interstory lateral displacement after the application of the complete time history of an earthquake and $D_y$ is defined, for all stories,

as the maximum interstory lateral displacement when the first plastic hinge is developed in the structure.

### 2.1.2. Global ductility ($\mu_G$)

Global ductility is defined as the mean value of the story ductility values.

## 3. Mathematical Formulation

Estimation of linear and nonlinear responses in time domain for three dimensional structures excited simultaneously by all the three components of an earthquake is essential to meet the objectives of the study. An assumed stress-based finite element algorithm, developed by the authors and their associates [25, 26], is used to estimate the nonlinear seismic responses of several steel building models. The procedure estimates the responses in time domain, as accurately as possible by considering material and geometry nonlinearities, and dissipation of energy. In this approach, an explicit form of the tangent stiffness matrix is derived without any numerical integration. Fewer elements can be used in describing a large deformation configuration without sacrificing any accuracy, and the material nonlinearity can be incorporated without losing its basic simplicity. The algorithm was implemented in a computer program. It gives very accurate results and is very efficient compared to the commonly used displacement-based approaches. The procedure and the algorithm have been extensively verified using available theoretical and experimental results [18, 19]. Since the concept is widely available in the literature and accepted by the profession, it is not presented here due to lack of space. Only the basic concept is presented here for the ready reference purpose.

The linear iterative strategy used to solve the nonlinear dynamic equation of motion can be expressed as:

$$\mathbf{m}\,^{(t+\Delta t)}\ddot{\mathbf{U}}^{(k)} + {}^{t}\mathbf{C}^{(t+\Delta t)}\dot{\mathbf{U}}^{(k)} + {}^{t}\mathbf{K}^{(t+\Delta t)}\Delta\mathbf{U}^{(k)} = {}^{(t+\Delta t)}\mathbf{F}^{(k)} - {}^{(t+\Delta t)}\mathbf{R}^{(k-1)} - \mathbf{m}\ddot{\mathbf{U}}_g^{(k)} \tag{1}$$

where $m$, $C$ and ${}^{t}K$ are the mass, damping and the tangent stiffness matrixes, respectively. $\ddot{U}$ and $\dot{U}$ are the acceleration and velocity vectors, respectively, $\Delta U$ is the incremental displacement vector, $F$ is the external load vector, $R$ is the internal force vector and $\ddot{U}_g$ is the ground acceleration vector. Superscripts $(t + \Delta t)$ and $(k)$ indicate the time and the iteration number, respectively. Rayleigh-type damping is commonly used for nonlinear analysis in the profession since it is a function of the mass and stiffness matrices representing the current state of a structure. Rayleigh-type damping is considered in this study. Explicit expressions for the tangent stiffness matrix and the internal force vector are developed for each beam-column element using the assumed stress-based finite element method for the $k^{th}$ iteration at time $t$. The nonlinear elastic tangent stiffness matrix for a beam-column element, $K^e$, can be represented as:

291

$$\mathbf{K}^e = \mathbf{A}_{\alpha lo}^T \mathbf{A}_{\sigma\sigma}^{-1} \mathbf{A}_{\alpha lo} + \mathbf{A}_{ddo} \tag{2}$$

where $A_{\sigma\sigma}^{-1}$ is the elastic property matrix, $A_{\alpha do}$ is the transformation matrix and $A_{ddo}$ is the geometric stiffness matrix. Similarly, the internal force vector of an element level, $R^e$, can be expressed as:

$$\mathbf{R}^e = -\mathbf{A}_{\alpha lo}^T \mathbf{A}_{\sigma\sigma}^{-1} \mathbf{R}_\sigma + \mathbf{R}_{do} \tag{3}$$

where $R_{do}$ is the homogeneous part of the internal force vector and $R_\sigma$ is the deformation difference vector. It is not possible to give explicit expressions for all the terms in Eqs. (2) and (3) due to lack of space, but they can be found in the literature.

The nonlinear structural behavior discussed above also needs to be modified to consider material nonlinearity. In this study, the material is considered to be linear elastic except at plastic hinges. Concentrated plasticity behavior is assumed at plastic hinge locations. For mathematical modeling, plastic hinges are assumed to occur at locations where the combined action of axial force, torsion, and bending moments satisfies a prescribed yield function. The yield function for three-dimensional beam-column elements and W-shape sections used in this study has the following form:

$$\left(\frac{P}{P_n}\right)^2 + \left(\frac{M_X}{M_{nX}}\right)^2 + \left(\frac{M_Y}{M_{nY}}\right)^2 + \left(\frac{M_Z}{M_{nZ}}\right)^2 - 1 = 0 \tag{4}$$

where $P$ is the axial force, $M_x$ and $M_y$ are the bending moments with respect to the major and minor axis, respectively, $M_z$ is the torsional moment, $P_n$ is the axial strength, $M_{nx}$ and $M_{ny}$ are the flexural strength with respect to the major and minor axis, respectively, and $M_{nz}$ is the torsional strength. The presence of plastic hinges in the structure will produce additional axial deformation and relative rotation in a particular element. Thus, the tangent stiffness matrix needs to be modified if plastic hinges form. The elasto-plastic tangent stiffness matrix $K_p$ and the elasto-plastic internal force vector $R_p$ can be obtained by modifying the corresponding elastic matrixes as:

$$\mathbf{K}_P^e = \mathbf{K}^e - \mathbf{A}_{\alpha lo}^T \mathbf{A}_{\sigma\sigma}^{-1} \mathbf{V}_P \mathbf{C}_P^T \mathbf{A}_{\alpha lo} \tag{5}$$

$$\mathbf{R}_P^e = \mathbf{A}_{\alpha lo}^T (\mathbf{A}_{\sigma\sigma}^{-1} \mathbf{V}_P \mathbf{C}_P^T - \mathbf{A}_{\sigma\sigma}^{-1}) \hat{\mathbf{R}}_\sigma + \mathbf{R}_{do} \tag{6}$$

In Eqs. (5) and (6), $V_P$, $C_P$ and $\hat{R}_\sigma$ can be shown to be:

$$\mathbf{V}_P = \left[ \frac{-\partial f}{\partial N}, \frac{-\partial f}{\partial M}\left(1 - \frac{x}{l}\right), \frac{-\partial f}{\partial M}\left(\frac{x}{l}\right) \right]^T \tag{7}$$

$$\mathbf{C}_P^T = \left(\mathbf{V}_P^T \mathbf{A}_{\sigma\sigma}^{-1}\right)^{-1} \mathbf{V}_P^{-1} \mathbf{A}_{\sigma\sigma}^{-1} \tag{8}$$

$$\bar{\mathbf{R}}_\sigma = \mathbf{R}_\sigma + \left\{ \begin{array}{c} H_P \\ \theta_P^*\left(1 - \dfrac{X}{l}\right) \\ \theta_P^*\left(\dfrac{X}{l}\right) \end{array} \right\} \tag{9}$$

$H_p$ and $\theta_P^*$ in Eq. (9) are the additional axial elongation and additional relative rotation at plastic hinges.

## 4. Structural Models

### 4.1. Buildings with PMRFs

Several steel model buildings were designed, as part of the SAC steel project, by three consulting firms. They considered 3-, 10- and 22- level buildings. The 10-level building has a single-level basement and the 20-level building has a 2-level basement. These buildings are supposed to satisfy all code requirements existed at the time of evaluation for the following three cities: Los Angeles (Uniform Building Code [12]), Seattle (Uniform building code [12]) and Boston (Building Officials & Code Administration ([27]). The 3- and 10- level buildings located in the Los Angeles area are considered in this study for numerical evaluations to address the issues discussed earlier. They will be denoted hereafter as Model SAC1 and SAC2, respectively and, in general, they will be referred as the SAC Models. They are considered to be bench mark models and have been used in many investigations. They provide a unique opportunity to study the behavior of steel buildings with perimeter MRSFs and interior GFs.

The elevations of the models are given in Figs. 1a and 1c and their plans are given in Figs. 1b and 1d, respectively. In these figures, the perimeter MRSFs are represented by continuous lines and the interior GFs are represented by dashed lines. For Model SAC2, the perimeter frames meet at a corner. In this case, the beam-to-column connections are considered to be pinned to eliminate weak axis bending (Fig. 1d). As can be seen, the buildings are essentially symmetrical in plan thus no significant torsional moments are expected to occur. Sizes of beams and columns, as reported by FEMA [1] , are given in Table 1 for the two models. The columns of the MRSFs of Model SAC1 are considered to be fixed at the base and pinned for Model SAC2, as considered in the FEMA report. In all these frames, the columns are made of steel Grade-50 and the girders are of A36 steel. For both models, the columns in the GFs are considered to be pinned at the base. All the columns in the perimeter MRSFs bend about the strong axis and the strong axes of the gravity columns are oriented in the N-S direction, as indicated in Figs. 1b and 1d. The designs of the MRSFs in the two orthogonal directions were practically the same. The first three translational periods of Models SAC1 and SAC2 for the N-S and E-W directions are given in Table 2. These periods were estimated by using the The Stodola Method which is included in the computer program mentioned in Section 3 of the paper. It is observed that for a

given model and the first mode, the translational periods are very close each other for the N-S and E-W direction. These periods match well with those reported in the FEMA report. Even though it was not explicitly calculated in this research, significant contribution is expected from the higher modes,

since their periods fall in the range of the predominant periods of the earthquakes. The damping is considered to be 5% of the critical damping; the value used in developing the code provisions in the U.S. Additional information for the models can be obtained from the FEMA report [1].
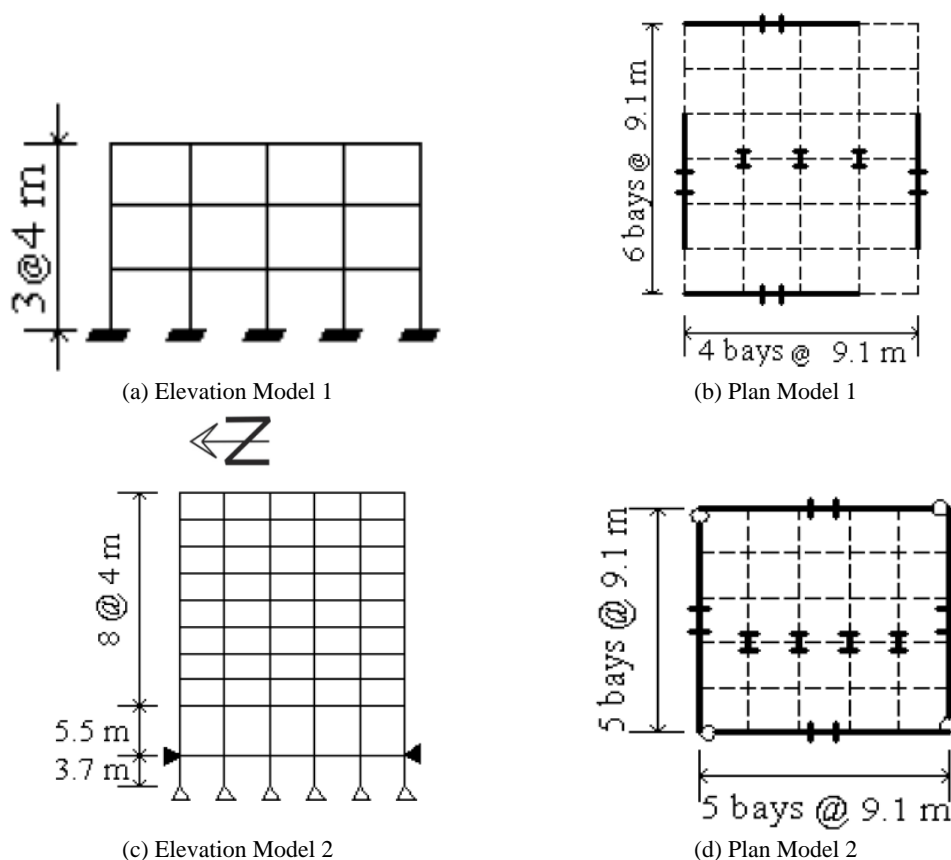


(a) Elevation Model 1        (b) Plan Model 1

(c) Elevation Model 2        (d) Plan Model 2

**Fig. 1** Elevations and plans for SAC1 and SAC2 Models

**Table 1** Beam and columns sections for SAC Models

| MODEL | STORY | MOMENT RESISTING FRAMES | | | GRAVITY FRAMES | | |
| | | COLUMNS | | GIRDERS | COLUMNS | | BEAMS |
| | | EXTERIOR | INTERIOR | | BELOW PENTHOUSE | OTHERS | |
|---|---|---|---|---|---|---|---|
| 3-LEVEL | 1\2 | W14x257 | W14x311 | W33X118 | W14x82 | W14x68 | W18x35 |
| | 2\3 | W14x257 | W14x312 | W30X116 | W14x82 | W14x68 | W18x35 |
| | 3\Roof | W14x257 | W14x313 | W24X68 | W14x82 | W14x68 | W16x26 |
| 10-LEVEL | -1/1 | W14x370 | W14x500 | W36x160 | W14x211 | W14x193 | W18x44 |
| | 1/2 | W14x370 | W14x500 | W36x160 | W14x211 | W14x193 | W18x35 |
| | 2/3 | W14x370 | W14x500,W14x455 | W36x160 | W14x211,W14x159 | W14x193,W14x145 | W18x35 |
| | 3/4 | W14x370 | W14x455 | W36x135 | W14x159 | W14x145 | W18x35 |
| | 4/5 | W14x370,W14x283 | W14x455,W14x370 | W36x135 | W14x159,W14x120 | W14x145,W14x109 | W18x35 |
| | 5/6 | W14x283 | W14x370 | W36x135 | W14x120 | W14x109 | W18x35 |
| | 6/7 | W14x283,W14x257 | W14x370,W14x283 | W36x135 | W14x120,W14x90 | W14x109,W14x82 | W18x35 |
| | 7/8 | W14x257 | W14x283 | W30x99 | W14x90 | W14x82 | W18x35 |
| | 8/9 | W14x257,W14x233 | W14x283,W14x257 | W27x84 | W14x90,W14x61 | W14x82,W14x48 | W18x35 |
| | 9/Roof | W14x233 | W14x257 | W24x68 | W14x61 | W14x48 | W16x26 |

The buildings are modeled as multi degree of freedom systems (MDOFs). Each column is represented by one element and each girder of the perimeter MRSFs is represented by two elements, having a node at the mid-span. The slab is modeled by near-rigid struts, as considered in the FEMA study [1] and it was implicitly assumed that the models have a strong panel zone. Each node is considered to have six degrees of freedom when the buildings are modeled in three dimensions while three degrees of freedom per node was considered for the bi-dimensional models.

## 4.2. Buildings with equivalent SMRFs

The equivalent models with SMRFs are designed by using an approximated procedure in such a way that, not only their fundamental period, total mass and lateral stiffness are fairly the same as those of the corresponding buildings with PMRFs, but also other characteristics to make the two structural "as equivalent" as possible, as stated below. The member properties of the equivalent buildings (EQ) are selected for one direction, say the *N-S* directions, and then in order to keep the equivalence, the same properties are assigned to the other direction. Two cases are considered for the equivalent models. In the first one, the sections of beam and columns of the SMRFs are selected by considering properties of the beams and columns of the perimeter MRSFs oriented in the direction under consideration. In the second case, the beam and columns are selected by additionally considering the perpendicular MRSFs. It must be noted that the columns of these frames bent with respect to their minor axis.

The mass per floor was the same for both systems, and to get a similar level of lateral stiffness for each interstory, the summation of the moments of inertia of all the columns, or girders, of the SAC models was approximately the same as the summation of the moments of inertia of all the columns of building with SMRFs. The ratios of moments of inertia of girders to those of columns, and the ratios of moments of inertia of interior columns to those of exterior columns, were also tried to keep as close as possible for the two structural systems. A Similar situation to that of moments of inertia applies for the plastic properties, to approximately have the same strength. For any interstory, the summation of the plastic axial loads (the product of the area and the yield stress) of the columns of the PMRF was approximately the same as the summation of the plastic axial loads of the columns of the models with SMRF. In the case of plastic moments, in order to keep the weak beam-strong column concept, the ratio of plastic moments of girders to plastic moments of columns was tried to keep as close as possible for the two structural systems.

The first equivalent models are referred, in general, as EQ1 Models and, in particular, as Model EQ11 and EQ12 for the 3- and 10-level buildings, respectively, while for the second case the model are referred, in general, as EQ2 models and, in particular, as Model EQ21 and EQ22 for the 3- and 10-level buildings. The resulting sections are shown in Table 3. As for the SAC models, the first three periods of the EQ1 and EQ2 models were estimated by using the The Stodola Method for both horizontal directions and presented in Table 2.

**Table 2** Translational periods for the SAC and equivalent models

| MODEL | DIRECTION | MODE NUMBER | | |
|---|---|---|---|---|
| | | 1 | 2 | 3 |
| SAC1 | N-S | 1.03 | 0.39 | 0.23 |
| | E-W | 0.99 | 0.36 | 0.18 |
| SAC2 | N-S | 2.30 | 0.82 | 0.50 |
| | E-W | 2.19 | 0.80 | 0.43 |
| EQ11 | N-S | 1.22 | 0.53 | 0.31 |
| | E-W | 1.15 | 0.48 | 0.26 |
| EQ12 | N-S | 2.50 | 0.78 | 0.50 |
| | E-W | 2.45 | 0.72 | 0.46 |
| EQ21 | N-S | 1.16 | 0.45 | 0.24 |
| | E-W | 1.09 | 0.41 | 0.18 |
| EQ22 | N-S | 2.43 | 0.90 | 0.48 |
| | E-W | 2.32 | 0.78 | 0.45 |

**Table 3** Beam and columns sections for the equivalent Models

| MODEL | STORY | EQ1 MODELS | | | EQ2 MODELS | | |
|---|---|---|---|---|---|---|---|
| | | COLUMNS | | GIRDERS | COLUMNS | | GIRDERS |
| | | EXTERIOR | INTERIOR | | EXTERIOR | INTERIOR | |
| 3-LEVEL | 1\2 | W14 X 74 | W14 X 90 | W24 X 55 | W16 X 67 | W14 X 109 | W12 X 170 |
| | 2\3 | W14 X 74 | W14 X 90 | W21 X 57 | W16 X 67 | W14 X 109 | W14 X 120 |
| | 3\Roof | W14 X 74 | W14 X 90 | W14 X 43 | W16 X 67 | W14 X 109 | W16 X 40 |
| 10-LEVEL | -1/1 | W14 X 159 | W14 X 211 | W27 X 94 | W18 X 143 | W21 X 166 | W24 X 162 |
| | 1/2 | W14 X 159 | W14 X 211 | W27 X 94 | W18 X 143 | W21 X 166 | W24 X 162 |
| | 2/3 | W14 X 159 | W14 X 211 | W27 X 94 | W18 X 143 | W21 X 166 | W24 X 162 |
| | 3/4 | W14 X 159 | W14 X 193 | W24 X 94 | W18 X 143 | W21 X 147 | W21 X 166 |
| | 4/5 | W14 X 159 | W14 X 193 | W24 X 94 | W18 X 143 | W21 X 147 | W21 X 166 |
| | 5/6 | W14 X 109 | W14 X 159 | W24 X 94 | W21 X 93 | W27 X 84 | W21 X 166 |
| | 6/7 | W14 X 109 | W14 X 159 | W24 X 94 | W21 X 93 | W27 X 84 | W21 X 166 |
| | 7/8 | W14 X 99 | W14 X 109 | W24 X 55 | W14 X 145 | W18 X 106 | W24 X 68 |
| | 8/9 | W14 X 99 | W14 X 109 | W21 X 50 | W14 X 145 | W18 X 106 | W12 X 152 |
| | 9/Roof | W14 X 90 | W14 X 99 | W16 X 45 | W24 X 62 | W18 X 97 | W16 X 67 |

*A. Reyes-Salazar, E. Bojorquez, J.L. Rivera-Salas, A. Lopez-Barraza, H.E. Rodriguez-lozoya*

It is observed that, even though it was tried to make the PMRF and SMRF models "as a equivalent as possible", some differences exist between their translational periods, particularly for the 3-level models. To compare to global lateral stiffness between the SAC and EQ models, pushover analysis are performed and the results are shown

in Figs. 2. For the 3-level and 10-level buildings, it is observed that the global initial lateral stiffness and the strength of the SAC model are larger than those of the EQ1 models which in turn are smaller than those of the EQ2 models. These characteristics are essentially the same for both horizontal directions.
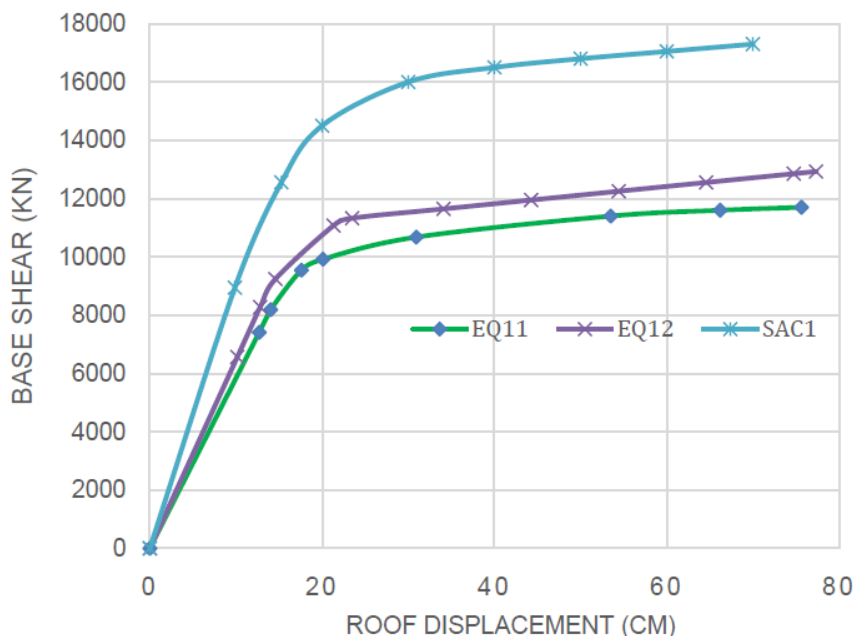


(a) 3- Level building
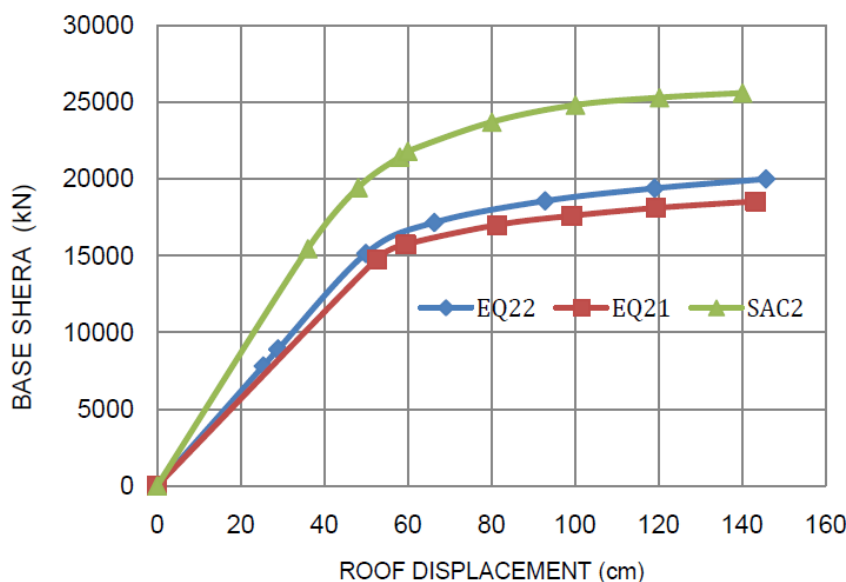


(b) 10- Level building
**Fig. 2** Pushover curves

### 4.3 Earthquake loading

Dynamic responses of a structure excited by different earthquake time histories, even when they are normalized with respect to the peak ground acceleration, are expected to be different reflecting their different frequency content. Thus, evaluating structural responses excited by an earthquake may not reflect the behavior properly. To study

the responses of the models comprehensively and to make meaningful conclusions, they are excited by twenty recorded earthquake motions in time domain with different frequency contents, recorded at different locations. First the earthquakes are scaled to the same PGA and then scaled in such a way that the models develop a significant level of plastic deformation. The characteristics of these earthquake time histories are given in Table 4. As shown in the table,

the predominant periods of the earthquakes vary from 0.11 to 1.0 sec. The predominant period for each earthquake is defined as the period where the largest peak in the elastic response spectrum occurs, in terms of pseudo accelerations. The earthquake time histories were obtained from the Data Sets of the National Strong Motion Program (NSMP) of the United States Geological Surveys (USGS). Additional information on these earthquakes can be obtained from these data base.

**Table 4** Earthquake models

| No | PLACE | YEAR | STATION | T (seg.) | ED (km) (Km) | M | PGA(mm/seg$^2$) |
|----|-------|------|---------|----------|--------------|---|-----------------|
| 1 | 1317 Mich. México | 1985 | Paraíso | 0.11 | 300 | 8.1 | 800 |
| 2 | 1634 Mammoth | 1980 | Mammoth H. S. Gym | 0.12 | 19 | 6.5 | 2000 |
| 3 | 1634 Mammoth Lakes | 1980 | Convict Creek | 0.19 | 18 | 6.5 | 3000 |
| 4 | 1317 Mich. México | 1985 | Infiernillo N-120 | 0.21 | 67 | 8.1 | 3000 |
| 5 | 1317 Mich. México | 1985 | La Unión | 0.32 | 121 | 8.1 | 1656 |
| 6 | 1733 El Salvador | 2001 | Relaciones Ext. | 0.34 | 96 | 7.8 | 2500 |
| 7 | 1733 El Salvador | 2001 | Relaciones Ext. | 0.41 | 95 | 7.8 | 1500 |
| 8 | 1634 Mammoth | 1980 | Long Valley Dam | 0.42 | 13 | 6.5 | 2000 |
| 9 | 2212 Delani Fault, AK | 2000 | K2-02 | 0.45 | 281 | 7.9 | 115 |
| 10 | 0836 Yountville CA | 2000 | Redwood City | 0.46 | 95 | 5.2 | 90 |
| 11 | 0408 Dillon MT | 2005 | MT:Kalispell | 0.51 | 338 | 5.6 | 51 |
| 12 | 1317 Mich. Mexico | 1985 | Villita | 0.53 | 80 | 8.1 | 1225 |
| 13 | 1232 Northrige | 1994 | Hall Valley | 0.54 | 25 | 6.4 | 2500 |
| 14 | 2115 Morgan Hill | 1984 | Hall Valley | 0.61 | 14 | 6.2 | 2000 |
| 15 | 2212 Delani Fault AK | 2002 | K2-04 | 0.62 | 290 | 7.9 | 133 |
| 16 | 0836 Yountville CA | 2000 | Dauville F.S. Ca | 0.63 | 73 | 5.2 | 144 |
| 17 | 0836 Yountville CA | 2000 | Pleasan Hill F.S. 1 | 0.71 | 92 | 5.2 | 74 |
| 18 | 0836 Yountville CA | 2000 | Pleasan Hill F.S. 2 | 0.75 | 58 | 5.2 | 201 |
| 19 | 2212 Delani Fault, AK | 2002 | Valdez City Hall | 0.85 | 272 | 7.9 | 260 |
| 20 | 1715 Park Fiel | 2004 | CA: Hollister City Hall | 1.01 | 147 | 6 | 145 |

## 5. Results in Terms of Interstory Shears

The seismic responses in terms of average interstory shears are estimated and compared for the different structural representations. The comparison is made for the twenty time history records, the 3- and 10-level buildings, elastic and inelastic behavior and for the *N-S* and *E-W* directions.
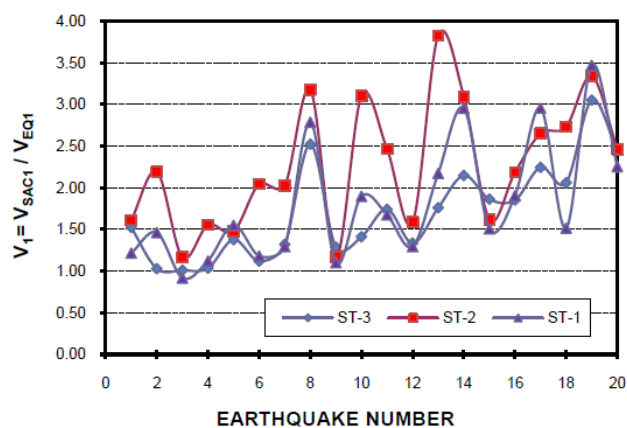
### 5.1 SAC and EQ1 models, elastic behavior

The average interstory shears are estimated for the SAC models and compared to those of their corresponding equivalent EQ1 models. The shear ratio $V_1$, defined as $V_{SAC1}/V_{EQ1}$, is introduced to make the comparison. For a given direction and story, $V_{SAC1}$ will represent the average interstory shear resisted by all the frames of the SAC models for the story under consideration and $V_{EQ1}$ will represent the same , but for the EQ1 models. All the earthquake time histories are normalized with respect to their maximum peak ground acceleration. The buildings remain essentially elastic when subjected to any of the earthquakes. The recorded seismic components are applied along the principal structural axes; the horizontal component with the major peak acceleration is applied in the *N-S* direction and the other in the *E-W* direction. The vertical component is also considered.

The results of the $V_1$ parameter are shown in Figs. 3a through 3d for the 3- and 10-level models and the *N-S* and *E-W* directions. The symbol *ST* is used in the figures to represent the word "story". It is observed that the $V_1$ values significantly vary from one earthquake to another and from one story to another without showing any trend, ranging from 0.8 to 3.8 and from 0.7 to 3.4 for the 3- and 10-level models, respectively. In general the $V_1$ values are larger for the *N-S* that for the *E-W*. The most important observation that can be made at this stage is that the $V_1$ parameter is larger than unity in most of the cases indicating that, in general, the interstory shears are larger for the buildings with PMRF. Values larger than 3 are obtained in some cases. One of the reasons for this is that, as shown in Table 2 and Fig. 2, the stiffness and strength of the buildings with PMRFs are larger than that of the buildings with SMRF. However, for many cases, $V_1$ takes values close to or slightly below unity indicating that the stiffness and the strength of the buildings are not the only parameters influencing the $V_1$ values. The broad variation of the magnitude of $V_1$ from one earthquake to another is also influenced by the differences between the dynamic properties of the buildings with PMRFs and SMRFs and by the frequency contents of the used motions. It is known

*A. Reyes-Salazar, E. Bojorquez, J.L. Rivera-Salas, A. Lopez-Barraza, H.E. Rodriguez-lozoya*

that the response of a building under dynamic loading is controlled by several parameters; among them we can mention the distribution of mass and stiffness, higher mode effects, frequency characteristics of the earthquakes and damping characteristics. Since the damping matrix is expressed as a combination of the mass and stiffness
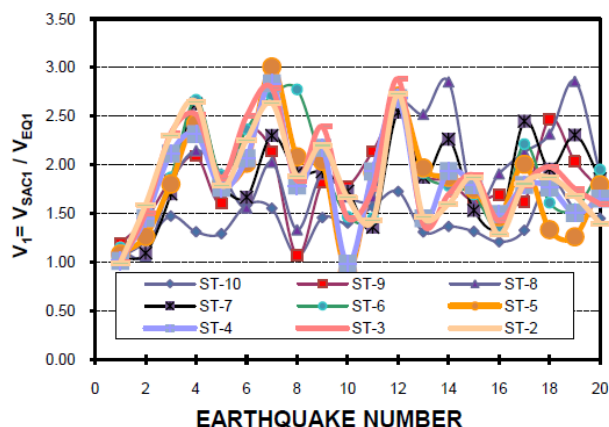
matrix, which are different for the two structural systems under consideration, the damping characteristics are expected to be different too. It is worth to mention that the maximum deformation of the buildings for each earthquake, in terms of maximum interstory displacements, was essentially the same.
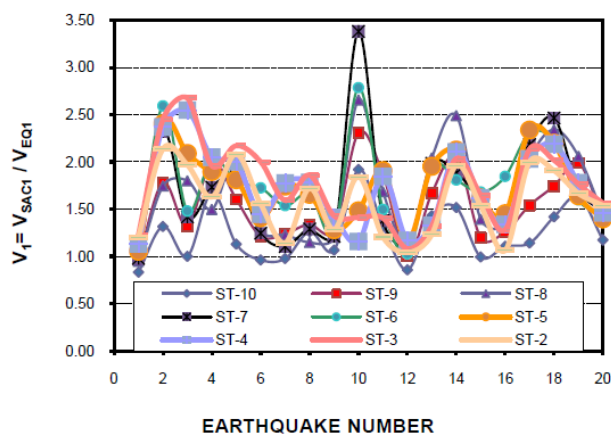


(a) 3-level model, *N-S* direction
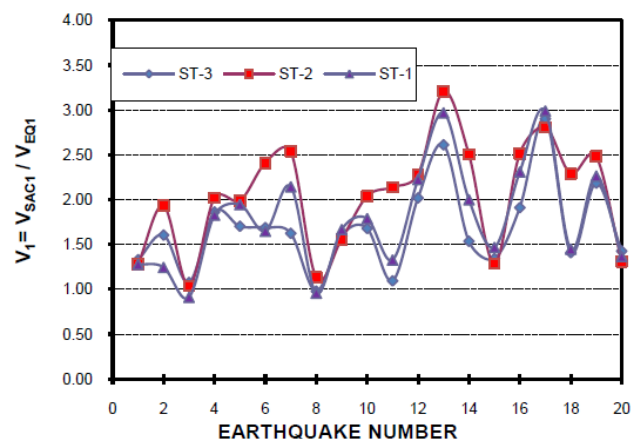
(b) 3-level model, *E-W* direction

(c) 10-level model, *N-S* direction
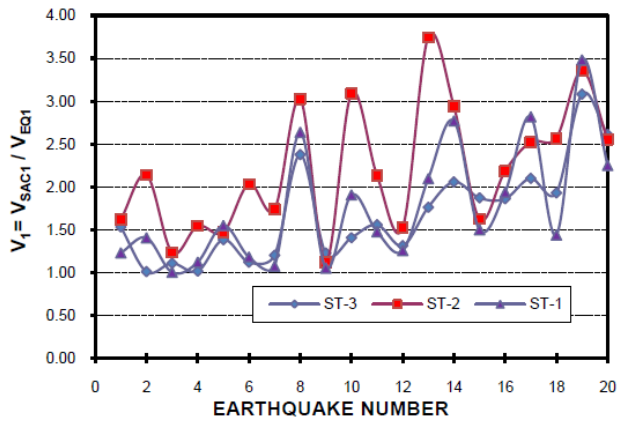
(d) 10-level model, *E-W* direction

**Fig. 3** Values of the $V_1$ parameter, elastic behavior

*5.2 SAC and EQ1 models, inelastic behavior*

To study the effect of inelastic behavior on the $V_1$ parameter, the actual time histories were scaled up so that yielding was produced in all the models. Based on the past experience and for the uniformity of comparison, all the actual time histories were scaled up to develop a maximum average interstory drift of about 2% by the trial and error procedure, instead of tracking the total number of plastic hinges developed. It was observed that about ten to twenty five plastic hinges were formed in the models when they developed the desired drift. Plots similar to those previously discussed are then developed; they are shown in Figs. 4a and 4d. As for the elastic behavior case, it is observed that the $V_1$ values significantly vary from one earthquake to another, from on model to another and from one story to another without showing any trend, that the $V_1$

values are larger for the *N-S* than for the *E-W* direction, and that they are larger than unity in practically all of the cases.

The values of $V_1$ are averaged over all the earthquakes, the statistics are summarized in Table 5 for both, elastic and inelastic behavior. As observed from individual plots, the statistics indicate that the interstory shears may be significantly larger for the buildings with perimeter MRSF. The mean values are similar for both models and levels of deformation (elastic and inelastic behavior), but they are larger for the *N-S* than for the *E-W* direction. The uncertainty in the estimation of $V_1$ in terms of the coefficient of variation (COV) is large in many cases, being quite similar for both models, levels of deformation and structural directions. Values of up to 0.40 are observed in some cases.

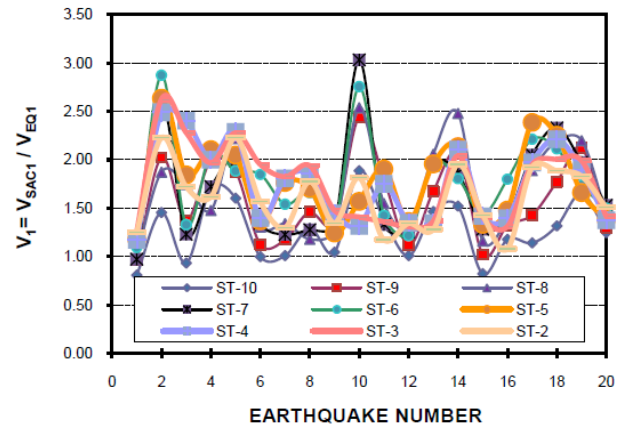(a) 3-level model, N-S direction          (b) 3-level model, E-W direction
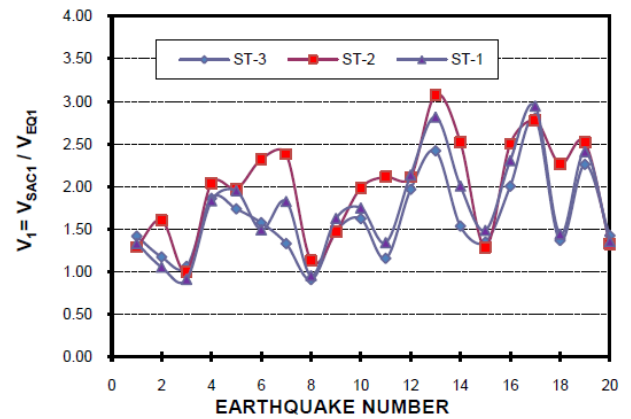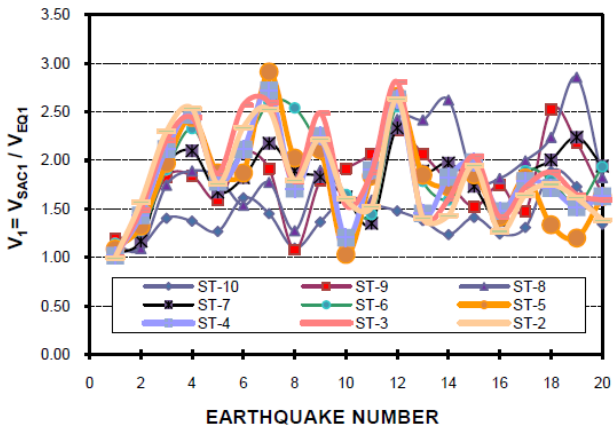
(c) 10-level model, *N-S* direction          (d) 10-level model, *E-W* direction

**Fig. 4** Values of the $V_1$ parameter, inelastic behavior

**Table 5** Statistics for the $V_1$ and $V_2$ ratios

| MODEL | | STORY | Statistics of $V_1$ | | | | | | Statistics of $V_2$ | | | | | |
|---|---|---|---|---|---|---|---|---|---|---|---|---|---|---|
| | | | *N-S* direction | | | *E-W* direction | | | *N-S* direction | | | *E-W* direction | | |
| | | | Mean | SD | CV | Mean | SD | CV | Mean | SD | CV | Mean | SD | CV |
| 3-LEVEL | ELASTIC | **3** | 1.71 | 0.57 | 0.33 | 1.68 | 0.48 | 0.29 | 1.12 | 0.14 | 0.13 | 1.15 | 0.09 | 0.08 |
| | | **2** | 2.27 | 0.77 | 0.34 | 2.04 | 0.60 | 0.30 | 0.99 | 0.09 | 0.09 | 0.97 | 0.08 | 0.08 |
| | | **1** | 1.81 | 0.73 | 0.40 | 1.79 | 0.58 | 0.32 | 0.98 | 0.10 | 0.10 | 1.03 | 0.11 | 0.11 |
| | INELASTIC | **3** | 1.68 | 0.57 | 0.34 | 1.62 | 0.48 | 0.30 | 1.13 | 0.14 | 0.12 | 1.15 | 0.11 | 0.10 |
| | | **2** | 2.21 | 0.75 | 0.34 | 1.98 | 0.59 | 0.30 | 0.98 | 0.09 | 0.10 | 0.97 | 0.09 | 0.09 |
| | | **1** | 1.76 | 0.71 | 0.40 | 1.75 | 0.57 | 0.33 | 0.97 | 0.10 | 0.10 | 1.04 | 0.10 | 0.10 |
| 10-LEVEL | ELASTIC | **10** | 1.40 | 0.20 | 0.14 | 1.24 | 0.29 | 0.24 | 1.05 | 0.20 | 0.19 | 1.08 | 0.20 | 0.19 |
| | | **9** | 1.85 | 0.39 | 0.21 | 1.54 | 0.38 | 0.24 | 1.29 | 0.23 | 0.18 | 1.24 | 0.28 | 0.22 |
| | | **8** | 1.95 | 0.51 | 0.26 | 1.67 | 0.49 | 0.29 | 1.36 | 0.27 | 0.20 | 1.33 | 0.27 | 0.20 |
| | | **7** | 1.87 | 0.45 | 0.24 | 1.68 | 0.58 | 0.34 | 1.31 | 0.28 | 0.21 | 1.37 | 0.32 | 0.23 |
| | | **6** | 1.92 | 0.51 | 0.26 | 1.76 | 0.46 | 0.26 | 1.40 | 0.26 | 0.19 | 1.43 | 0.37 | 0.26 |
| | | **5** | 1.82 | 0.52 | 0.29 | 1.73 | 0.38 | 0.22 | 1.36 | 0.26 | 0.19 | 1.44 | 0.29 | 0.20 |
| | | **4** | 1.83 | 0.47 | 0.26 | 1.73 | 0.42 | 0.24 | 1.39 | 0.33 | 0.24 | 1.42 | 0.31 | 0.22 |
| | | **3** | 1.92 | 0.50 | 0.26 | 1.75 | 0.43 | 0.24 | 1.46 | 0.32 | 0.22 | 1.40 | 0.34 | 0.24 |
| | | **2** | 1.85 | 0.48 | 0.26 | 1.59 | 0.36 | 0.23 | 1.41 | 0.31 | 0.22 | 1.28 | 0.33 | 0.26 |
| | | **10** | 1.79 | 0.37 | 0.21 | 1.57 | 0.42 | 0.27 | 1.08 | 0.21 | 0.19 | 1.03 | 0.22 | 0.21 |
| | | **9** | 1.87 | 0.46 | 0.25 | 1.68 | 0.47 | 0.28 | 1.32 | 0.27 | 0.20 | 1.23 | 0.31 | 0.26 |
| | | **8** | 1.80 | 0.34 | 0.19 | 1.68 | 0.53 | 0.32 | 1.34 | 0.32 | 0.24 | 1.29 | 0.28 | 0.22 |
| | | **7** | 1.87 | 0.42 | 0.22 | 1.78 | 0.47 | 0.26 | 1.32 | 0.32 | 0.24 | 1.35 | 0.35 | 0.26 |

*A. Reyes-Salazar, E. Bojorquez, J.L. Rivera-Salas, A. Lopez-Barraza, H.E. Rodriguez-lozoya*

| | | | | | | | | | | | | | |
|---|---|---|---|---|---|---|---|---|---|---|---|---|---|
| INELASTIC | 6 | 1.80 | 0.50 | 0.28 | 1.77 | 0.41 | 0.23 | 1.39 | 0.30 | 0.22 | 1.39 | 0.34 | 0.25 |
| | 5 | 1.84 | 0.45 | 0.25 | 1.75 | 0.41 | 0.23 | 1.33 | 0.28 | 0.21 | 1.43 | 0.31 | 0.21 |
| | 4 | 1.90 | 0.48 | 0.25 | 1.76 | 0.40 | 0.23 | 1.39 | 0.34 | 0.25 | 1.39 | 0.32 | 0.23 |
| | 3 | 1.81 | 0.46 | 0.26 | 1.61 | 0.34 | 0.21 | 1.48 | 0.38 | 0.25 | 1.40 | 0.32 | 0.23 |
| | 2 | 1.79 | 0.37 | 0.21 | 1.57 | 0.42 | 0.27 | 1.41 | 0.36 | 0.26 | 1.26 | 0.33 | 0.26 |

## 5.3 SAC and EQ2 models, elastic and inelastic behavior

The comparison between the interstory shears of the SAC1 and the EQ2 models is made in terms of the $V_2$ parameter which is defined as $V_{SAC1}/V_{EQ2}$. For a given direction and story, $V_{EQ2}$ will represent the average interstory shear resisted by all the frames of the EQ2 models for the story under consideration, $V_{SAC1}$ was defined before. Similar plots to those of $V_1$ are also developed for $V_2$, but only those of the 10-level building and elastic behavior are presented (Figs 5a and 5b). The statistics, however, are presented in Table 5 for all the cases. Many of the observations made for the $V_1$ ratio also apply to $V_2$. The only additional observations that can be mentioned are that the mean values of $V_2$ and the uncertainty in the estimation may be significantly larger for the 10- than for the 3-level building and that they are quite similar for both structural directions. It is also observed that the mean and COV of $V_2$ are in general smaller than those of $V_1$. It indicates that the interstory shears increase as the stiffness of the steel building with SMRFs increases and consequently considering the perpendicular MRSFs in the design of the equivalent models has an important effect on their structural response.
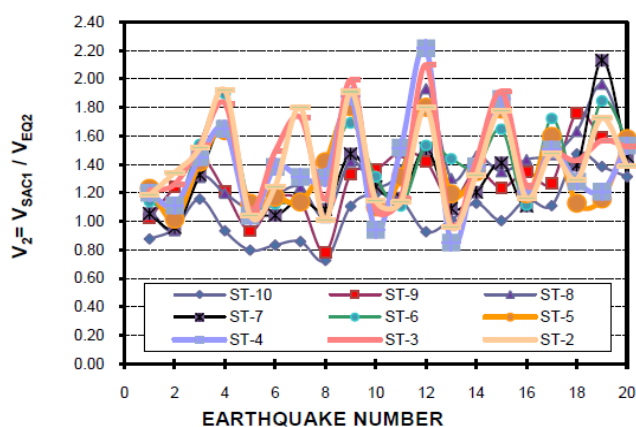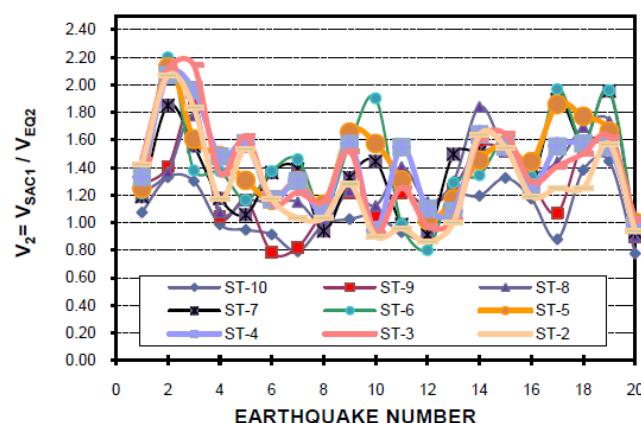


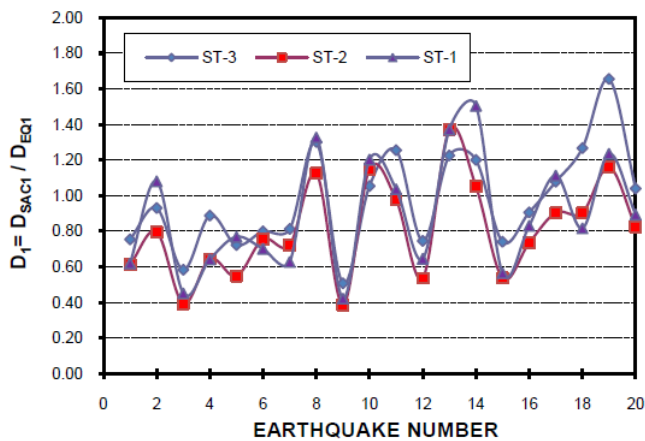(a) 10-level model, *N-S* direction          (b) 10-level model, *E-W* direction

**Fig. 5** Values of the $V_2$ parameter, elastic behavior

## 6. Results in Terms of Interstory Displacements

### 6.1. SAC and EQ1 models, elastic behavior

The $D_1$ parameter is used to compare the interstory displacements of the *SAC* models with those of the EQ1 models. $D_1$ is defined as $D_{SAC1}/D_{EQ1}$ where the terms of this ratio have a similar meaning than those of the case of shear, except that they now represent interstory displacements. The values of $D_1$ are given in Figs 6a through 6d. The results resemble those of interstory shears in the sense that the values significantly vary without showing any trend, but they are different in another sense since the values of these parameters are smaller than unity in most of the cases indicating that the interstory displacements are larger for the buildings with SMRFs. The reasons for these differences are, as stated in Section 5.1, the lower flexibility of the buildings with SMRFs and the different dynamic properties of the structural systems, in terms of stiffness distribution, high modal contribution and damping characteristics. The differences in the response of the two structural systems, however, are much larger for the case of shears than for displacements.
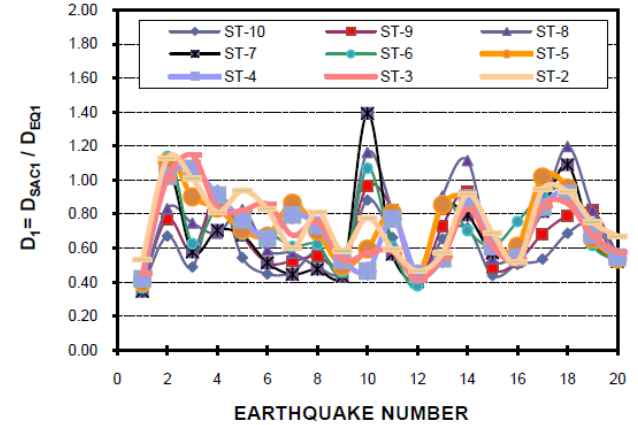
(a) 3-level model, N-S direction
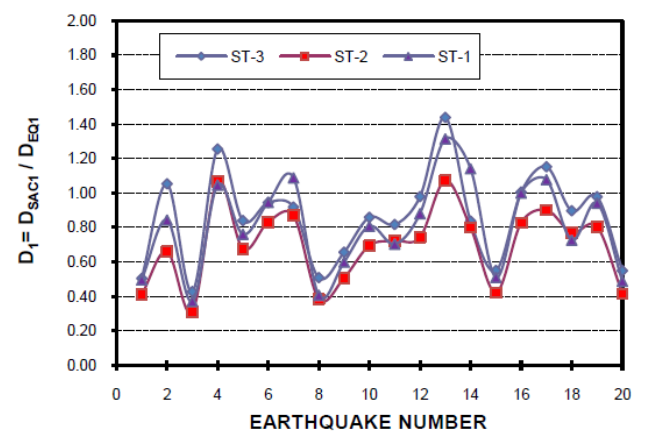


(b) 3-level model, E-W direction
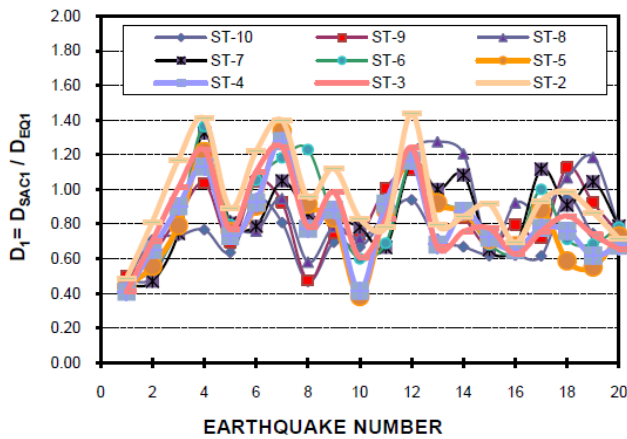


(c) 10-level model, *N-S* direction



(d) 10-level model, *E-W* direction

**Fig. 6** Values of the $D_1$ parameter, elastic behavior

*6.2. SAC and EQ1 models, inelastic behavior*

Plots of $D_1$ for inelastic behavior are also developed but are not shown, only their statistics are discussed. They are presented in Table 6 for both, elastic and inelastic behavior. The statistics for the elastic case confirmed what

observed for individual plots: the interstory displacements are larger for the buildings with SMRFs. It is observed that the mean values and the uncertainty in the estimation are larger for the 3- than for the 10-level model, but they are quite similar for elastic and inelastic behavior.

**Table 6** Statistics for the $D_1$ and $D_2$ parameters

| MODEL | | STORY | Statistics of $D_1$ | | | | | | Statistics of $D_2$ | | | | | |
| | | | N-S direction | | | E-W direction | | | N-S direction | | | E-W direction | | |
| | | | Mean | SD | CV | Mean | SD | CV | Mean | SD | CV | Mean | SD | CV |
| 3-LEVEL | ELASTIC | **3** | 0.97 | 0.28 | 0.29 | 0.86 | 0.27 | 0.31 | 1.49 | 0.17 | 0.12 | 1.43 | 0.11 | 0.08 |
| | | **2** | 0.81 | 0.27 | 0.34 | 0.69 | 0.22 | 0.32 | 1.11 | 0.08 | 0.07 | 1.08 | 0.08 | 0.08 |
| | | **1** | 0.89 | 0.32 | 0.36 | 0.81 | 0.27 | 0.33 | 0.63 | 0.07 | 0.11 | 0.65 | 0.07 | 0.10 |
| | INELASTIC | **3** | 0.96 | 0.26 | 0.27 | 0.87 | 0.27 | 0.31 | 1.55 | 0.21 | 0.14 | 1.48 | 0.16 | 0.11 |
| | | **2** | 0.81 | 0.27 | 0.33 | 0.70 | 0.21 | 0.31 | 1.15 | 0.11 | 0.10 | 1.11 | 0.12 | 0.10 |
| | | **1** | 0.89 | 0.34 | 0.38 | 0.80 | 0.26 | 0.33 | 0.62 | 0.09 | 0.14 | 0.67 | 0.08 | 0.12 |
| 10-LEVEL | ELASTIC | **10** | 0.71 | 0.13 | 0.19 | 0.59 | 0.16 | 0.27 | 0.75 | 0.14 | 0.18 | 0.74 | 0.16 | 0.21 |
| | | **9** | 0.83 | 0.19 | 0.23 | 0.66 | 0.18 | 0.27 | 0.83 | 0.16 | 0.19 | 0.78 | 0.18 | 0.24 |
| | | **8** | 0.88 | 0.24 | 0.28 | 0.73 | 0.24 | 0.33 | 0.88 | 0.17 | 0.19 | 0.83 | 0.19 | 0.23 |
| | | **7** | 0.86 | 0.23 | 0.27 | 0.67 | 0.26 | 0.39 | 0.87 | 0.18 | 0.21 | 0.81 | 0.19 | 0.23 |
| | | **6** | 0.85 | 0.25 | 0.29 | 0.70 | 0.21 | 0.30 | 0.91 | 0.18 | 0.20 | 0.85 | 0.23 | 0.27 |
| | | **5** | 0.81 | 0.25 | 0.31 | 0.73 | 0.19 | 0.26 | 0.86 | 0.17 | 0.19 | 0.87 | 0.19 | 0.22 |
| | | **4** | 0.80 | 0.22 | 0.28 | 0.71 | 0.19 | 0.27 | 0.88 | 0.22 | 0.25 | 0.84 | 0.20 | 0.23 |
| | | **3** | 0.84 | 0.23 | 0.27 | 0.71 | 0.19 | 0.27 | 0.95 | 0.21 | 0.22 | 0.83 | 0.20 | 0.25 |

|  |  |  |  |  |  |  |  |  |  |  |  |  |
|---|---|---|---|---|---|---|---|---|---|---|---|---|
|  | **2** | 0.96 | 0.26 | 0.26 | 0.75 | 0.19 | 0.25 | 1.11 | 0.25 | 0.22 | 0.90 | 0.23 | 0.25 |
|  | **10** | 0.70 | 0.13 | 0.19 | 0.60 | 0.18 | 0.29 | 0.76 | 0.15 | 0.19 | 0.74 | 0.22 | 0.30 |
|  | **9** | 0.80 | 0.20 | 0.25 | 0.69 | 0.21 | 0.30 | 0.81 | 0.16 | 0.20 | 0.78 | 0.22 | 0.28 |
|  | **8** | 0.84 | 0.28 | 0.33 | 0.76 | 0.27 | 0.36 | 0.82 | 0.20 | 0.24 | 0.85 | 0.21 | 0.24 |
|  | **7** | 0.83 | 0.25 | 0.30 | 0.68 | 0.29 | 0.43 | 0.83 | 0.22 | 0.27 | 0.81 | 0.18 | 0.22 |
| INELASTIC | **6** | 0.84 | 0.26 | 0.31 | 0.71 | 0.25 | 0.36 | 0.91 | 0.24 | 0.26 | 0.83 | 0.20 | 0.25 |
|  | **5** | 0.80 | 0.24 | 0.30 | 0.74 | 0.20 | 0.28 | 0.88 | 0.21 | 0.24 | 0.88 | 0.20 | 0.23 |
|  | **4** | 0.80 | 0.21 | 0.26 | 0.70 | 0.20 | 0.29 | 0.87 | 0.24 | 0.28 | 0.85 | 0.22 | 0.26 |
|  | **3** | 0.85 | 0.23 | 0.27 | 0.71 | 0.20 | 0.29 | 0.96 | 0.24 | 0.25 | 0.83 | 0.21 | 0.26 |
|  | **2** | 0.97 | 0.28 | 0.29 | 0.76 | 0.20 | 0.26 | 1.11 | 0.29 | 0.26 | 0.91 | 0.24 | 0.26 |

### 6.3. SAC and EQ2 models, elastic and inelastic behavior

The comparison between the interstory displacements of the SAC1 and the EQ2 models is made by using the $D_2$ parameter which is defined as $D_{SAC1}/D_{EQ2}$. Plots for $D_2$ are developed but are not shown, only the statistics are discussed (Table 6). Results of the table indicate that, for the 3-level model the $D_2$ mean values are larger than unity in most of the cases. For the 10-level building, however, in general, the mean values of $D_2$ are smaller than unity in most of the cases indicating that the values of the interstory displacements are smaller for the EQ2 models. The mean values quite similar for elastic and inelastic behavior. The explanation for this is that the fundamental period of the 3-level systems fall close to the short period zone of the spectra, and in this zone, a smaller lateral strength implies larger lateral displacements. On the other hand, the 10-level building has a fundamental period of vibration away from the corner period of the ground motions. It is also observed that the uncertainty in the estimation of $D_2$ is similar for elastic and inelastic behavior, but larger for the 10- than for the 3-level model. Unlike the case of the comparison of the $V_1$ and $V_2$ parameters, the mean values of the $D_1$ and $D_2$ ratios are quite similar.

## 7. Results in Terms of Ductility

### 7.1. Story ductility (μ)

The results in terms of story ductility demands are estimated for all the structural systems under consideration and compared each other in this section of the paper. The ratios $\mu_{1=}\mu_{SAC/}\mu_{EQ1}$ and $\mu_{2=}\mu_{SAC/}\mu_{EQ2}$ are used for this purpose. The parameters $\mu_{SAC}$, $\mu_{EQ1}$ and $\mu_{EQ2}$ represent the story ductility demands for the SAC, EQ1 and EQ2 models, respectively. The results for the $\mu_1$ ratio are presented in Figs. 7a through 7d, for the *N-S* and *E-W* directions and the 3- and 10-level buildings. As for the case of the $D_1$, $D_2$, $V_1$ and $V_2$ parameters, the $\mu_1$ ratio varies from one earthquake to another and from one story to another. The values are observed to be larger for the 3- than for the 10-level building. The most important observation that can be made is that the values of $\mu_1$ are, in general, larger than unity in most of the cases indicating that the ductility demands are larger for the steel buildings with PMRF; values larger than 3 are reached in many cases. The implication of this is that, since larger ductility demands are imposed on the building with PMRFs for the same level of earthquake loading, the detailing of the connections of this structural system will have to be more stringent than for the building with SMRFs.
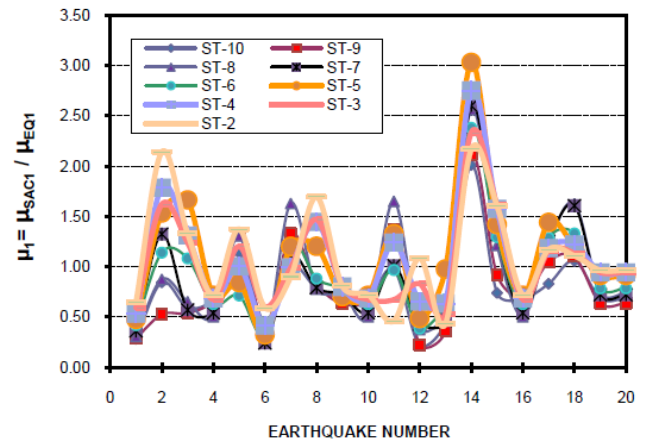


(a) 3-level model, *N-S* direction



(b) 3-level model, *E-W* direction

301
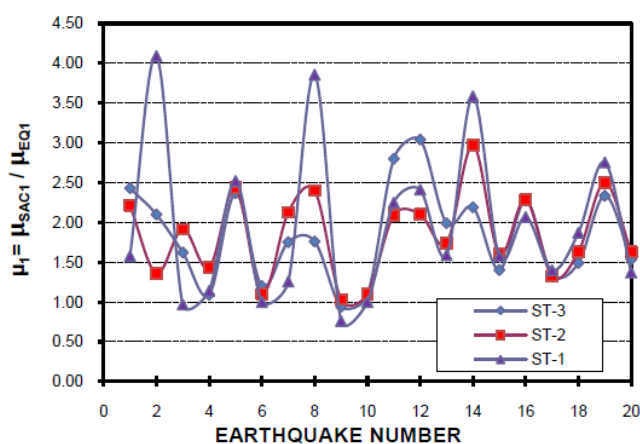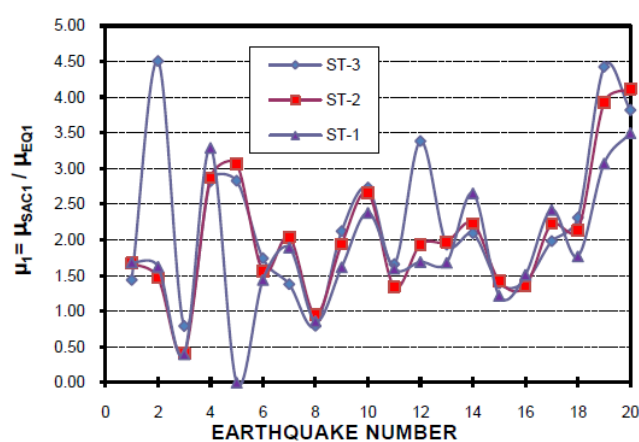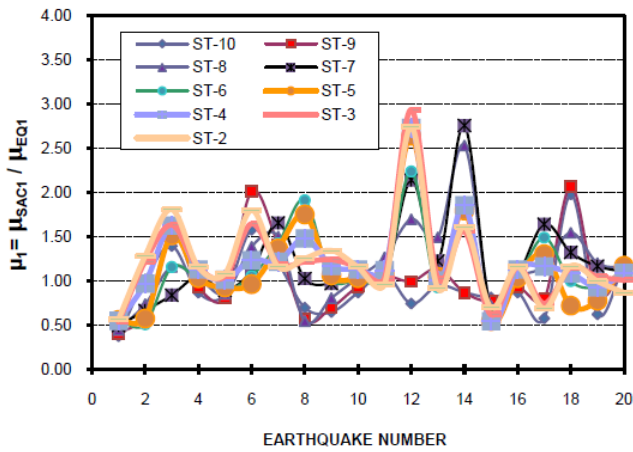
(c) 10-level model, *N-S* direction      (d) 10-level model, *E-W* direction

**Fig. 7** Values of the $\mu_1$ parameter

The statistics of $\mu_1$ are presented in Table 7. As commented before for individual plots, it is observed that, in general, the mean values are larger that unity and larger for the 3- than for the 10-level building. For the 3-level building the mean values are larger for the *E-W* direction while for the 10-level building they are larger for the *N-S* direction. The uncertainty in the estimation is large with values of COV of up to 0.60 in some cases and it is larger for the *E-W* direction. Similar plots to those of $\mu_1$ are also developed for $\mu_2$, but are not shown, only their statistics

are discussed (Table 7). As for the case of the $\mu_1$ ratio, the mean values of $\mu_2$ are larger than unity in most of the cases, indicating again that the ductility demands are larger for the building with PMRFs. However, the $\mu_1$ mean values are larger for the 3-level building while for the case of $\mu_2$ resulted larger for the 10-level building. The uncertainty in the estimation of $\mu_2$ is similar for the 3- and 10-level buildings, but larger, in general, for the *E-W* than for the *N-S* direction.

**Table 7** Statistics for the $\mu_1$ and $\mu_2$ parameters

| MODEL | STORY | Statistics of $\mu_1$ | | | | | | Statistics of $\mu_2$ | | | | | |
| | | *N-S* direction | | | *E-W* direction | | | *N-S* direction | | | *E-W* direction | | |
| | | Mean | SD | CV | Mean | SD | CV | Mean | SD | CV | Mean | SD | CV |
| | 3 | 1.84 | 0.59 | 0.32 | 2.28 | 1.08 | 0.48 | 0.94 | 0.22 | 0.2 | 1.17 | 0.46 | 0.39 |
| 3-LEVEL | 2 | 1.85 | 0.54 | 0.29 | 2.06 | 0.92 | 0.44 | 1.01 | 0.18 | 0.1 | 1.08 | 0.23 | 0.22 |
| | 1 | 1.95 | 0.99 | 0.51 | 1.92 | 0.78 | 0.41 | 1.06 | 0.34 | 0.3 | 1.09 | 0.28 | 0.26 |
| | 10 | 0.96 | 0.37 | 0.39 | 0.77 | 0.38 | 0.48 | 1.42 | 0.46 | 0.3 | 1.34 | 0.51 | 0.38 |
| | 9 | 1.03 | 0.44 | 0.42 | 0.82 | 0.46 | 0.56 | 1.35 | 0.36 | 0.2 | 1.38 | 0.51 | 0.37 |
| | 8 | 1.17 | 0.47 | 0.40 | 0.94 | 0.58 | 0.62 | 1.29 | 0.32 | 0.2 | 1.49 | 0.55 | 0.37 |
| | 7 | 1.20 | 0.52 | 0.44 | 0.89 | 0.55 | 0.61 | 1.35 | 0.39 | 0.2 | 1.18 | 0.34 | 0.29 |
| 10-LEVEL | 6 | 1.14 | 0.45 | 0.39 | 1.02 | 0.46 | 0.45 | 1.39 | 0.36 | 0.2 | 1.19 | 0.31 | 0.26 |
| | 5 | 1.15 | 0.50 | 0.43 | 1.09 | 0.59 | 0.54 | 1.35 | 0.35 | 0.2 | 1.41 | 0.44 | 0.31 |
| | 4 | 1.21 | 0.47 | 0.38 | 1.07 | 0.54 | 0.50 | 1.38 | 0.45 | 0.3 | 1.42 | 0.48 | 0.34 |
| | 3 | 1.22 | 0.50 | 0.41 | 1.04 | 0.45 | 0.44 | 1.42 | 0.39 | 0.2 | 1.24 | 0.39 | 0.31 |
| | 2 | 1.22 | 0.49 | 0.40 | 1.08 | 0.51 | 0.47 | 1.41 | 0.39 | 0.2 | 1.17 | 0.40 | 0.34 |

*7.2 Global ductility ($\mu_G$)*

The values of global ductility, as defined earlier, are calculated and presented in Table 8. In this table, $\mu_{G1}$ represents the ratios of global ductility of the SAC and EQ1 models while $\mu_{G2}$ represents the same ratio for the SAC and EQ2 models. The results confirm what concluded from the discussion of story ductility demands:

the global ductility demands are, in general, larger for the structural buildings with PMRFs. This difference is more significant for the 3-story building of the SAC and EQ1 models ($\mu_{G1}$) while it is more significant for the 10-level building for the case of the SAC and EQ2 models ($\mu_{G2}$). The uncertainty in the estimation of global ductility ratios is larger for the $\mu_{G1}$ than for $\mu_{G2}$ parameter.

**Table 8** Values of the $\mu_{G1}$ and $\mu_{G2}$ parameters

| EARTHQUAKE | $\mu_{G1}$ | | | | $\mu_{G2}$ | | | |
| --- | --- | --- | --- | --- | --- | --- | --- | --- |
| | 3-LEVEL | | 10-LEVEL | | 3-LEVEL | | 10-LEVEL | |
| | N-S | E-W | N-S | E-W | N-S | E-W | N-S | E-W |
| 1 2 | 2.08 | 1.59 | 0.48 | 0.41 | 2.11 | 1.48 | 2.27 | 1.41 |
| 2 | 2.26 | 2.42 | 0.78 | 1.19 | 1.01 | 1.79 | 1.33 | 2.12 |
| 3 | 1.46 | 0.48 | 1.37 | 0.94 | 0.74 | 1.37 | 1.12 | 1.28 |
| 4 | 1.22 | 3.00 | 5.67 | 6.28 | 0.65 | 0.69 | 1.50 | 1.45 |
| 5 | 2.44 | 2.61 | 0.91 | 1.04 | 1.32 | 1.31 | 0.98 | 1.22 |
| 6 | 1.10 | 1.58 | 1.37 | 0.38 | 0.91 | 0.99 | 0.88 | 0.63 |
| 7 | 1.67 | 1.76 | 1.34 | 1.15 | 0.82 | 0.75 | 1.32 | 0.77 |
| 8 | 2.53 | 0.87 | 1.08 | 1.00 | 0.92 | 0.88 | 1.07 | 1.33 |
| 9 | 0.92 | 1.89 | 0.95 | 0.67 | 1.05 | 0.71 | 1.70 | 3.51 |
| 10 1 | 1.06 | 2.59 | 5.69 | 1.22 | 0.87 | 0.91 | 1.31 | 1.55 |
| 11 | 2.34 | 1.52 | 1.07 | 1.02 | 1.42 | 1.42 | 1.72 | 1.32 |
| 12 | 2.49 | 2.32 | 1.85 | 0.42 | 1.00 | 1.09 | 1.62 | 1.04 |
| 13 | 1.77 | 1.86 | 1.08 | 0.54 | 0.89 | 0.87 | 1.44 | 0.94 |
| |4 | 2.93 | 2.33 | 1.57 | 2.41 | 1.24 | 1.49 | 1.50 | 2.55 |
| 15 | 1.52 | 1.35 | 0.66 | 1.25 | 1.03 | 1.02 | 1.03 | 1.25 |
| 16 | 2.22 | 1.43 | 5.77 | 1.87 | 0.96 | 1.13 | 1.43 | 1.35 |
| 17 | 1.35 | 2.21 | 0.95 | 1.15 | 0.54 | 1.12 | 1.36 | 1.04 |
| 18 | 1.66 | 2.07 | 1.32 | 1.24 | 0.96 | 0.90 | 1.39 | 1.13 |
| 19 | 2.52 | 3.81 | 0.90 | 0.47 | 1.04 | 0.56 | 1.67 | 2.53 |
| 20 | 1.50 | 3.81 | 1.10 | 0.27 | 0.91 | 0.94 | 1.26 | 0.57 |
| **Mean** | **1.85** | **2.07** | **1.80** | **1.25** | **1.00** | **1.08** | **1.40** | **1.45** |
| **SD** | **0.58** | **0.85** | **1.72** | **1.30** | **0.33** | **0.32** | **0.34** | **0.78** |
| **CV** | **0.32** | **0.41** | **0.96** | **1.04** | **0.33** | **0.30** | **0.25** | **0.54** |

## 8. Conclusions

The linear and nonlinear responses of steel buildings with perimeter moment resisting frames (PMRFs) are estimated and compared with the corresponding responses of buildings with equivalent spatial moment resisting frames (SMRFs). The equivalent models with SMRFs are designed by using an approximated procedure in such a way that, not only their fundamental period, total mass and lateral stiffness are fairly the same as those of the corresponding buildings with PMRFs, but also other characteristics to make the two structural "as equivalent" as possible, as stated below. The mass was the same for both structural systems and the stiffness and strength as close as possible. The ratio of moments of inertia, or plastic moments, between beams and columns was approximately the same for the two structural systems. The same was considered for the case of interior and exterior columns. The comparison is expressed in terms of interstory shears, interstory displacements and ductility. The numerical study indicates that the interstory shears of the buildings with PMRFs may be significantly larger than those of the buildings with SMRFs. One of the main reasons for this is that the buildings with PMRFs are stiffer than the buildings with SMRFs. However, for many cases the shears are slightly larger for the buildings with SMRF . The broad variation of shears from one earthquake to another is also influenced by the differences between the dynamic properties of the two types of buildings and by the frequency contents of the used motions. Unlike the case of interstory shears, the interstory displacements are similar for both structural systems in many cases. For some other cases, however, they are larger for the model with SMRFs, depending upon the closeness between the earthquake corner periods and the periods of the buildings. The differences, however, are much larger for the case of shears than for displacements. The global and story ductility demands are, in general, larger for the steel buildings with perimeter moment resisting steel frames. The implication of this is that, since larger ductility demands are imposed on the building with PMRFs for the same level of earthquake loading, the detailing of the connections of this structural system will have to be more stringent than for the building with SMRFs, proper detailing of connections has to be taken into account too in order the get the required rotations It can be concluded, that the seismic performance of the steel buildings with SMRFs may be superior to that of steel buildings with PMRFs. The findings of this paper are for the particular models used in the study. Much more research is needed to reach more general conclusions.

## References

[1]     FEMA (355C), State of the Art Report on Systems Performance of Steel Moment Frames Subjected to Earthquake Ground Shaking, SAC Steel Project, Report FEMA 355C, Federal Emergency Management Agency, 2000.

[2]     Rentschler GP, Chen WF, Driscoll GC. Tests of beam-to-column web moment connections, Journal of the Structural Division, ASCE, 1980, No. 5, Vol. 106, pp. 1005-1022.

[3]     Reyes-Salazar A, Bojórquez , López-Barraza A, De Leon-Escobedo D, Haldar A. Some issues regarding the structural idealization of perimeter moment resisting steel frames, ISET Journal of Earthquake Technology, 2009, Nos. 3-4, Vol. 46, pp. 133-146.

[4]     Mele E, Di Sarno L, De Luca A. Seismic behavior of perimeter and spatial steel frames, Journal of Earthquake Engineering, 2004, No. 3, 8, pp. 457-496.

[5]     FEMA (350). Recommended Seismic Design Criteria for New Steel Moment-Frame Building, SAC Steel Project, Report FEMA 350, Federal Emergency Management Agency, 2000.

[6]     Reglamento de construcciones del Distrito Federal, Normas Técnicas Complementarias de Diseño por Sismo, Gaceta Oficial del Distrito Federal, 2004.

[7]     Lee K, Foutch DA. Performance evaluation of new steel frame buildings for seismic loads, Earthquake Engineering and Structural Dynamics, 2001, No. 3, Vol. 31, pp. 653-670.

[8]     Foutch A, Yun SY. Modeling of steel moment frames for seismic loads, Journal of Constructional Steel Research, 2002, Vol. 58, pp. 529-564.

[9]     Gupta A, Krawinkler H. Behavior of ductile SMRFs at various seismic hazard levels, Journal of Structural Engineering, 2000, No. 1, Vol. 126, pp. 98-107.

[10]    Lee K, Foutch DA. Seismic evaluation of steel moment frames buildings designed using different r-values, Journal of Structural Engineering Division, ASCE, 2006, No. 9, Vol. 132, pp. 1461-1472.

[11]    Krishnan S, Ji C, Komatitsch D, Tromp J. Performance of two 18-storey steel moment-frame building in southern California during two large simulated San Andres Earthquakes, Earthquake Spectra, 2006, No. 4, Vol. 22, pp. 1035-1061.

[12]    UBC, Structural Engineering Design Provisions, Uniform Building Code, International Conference of Building Officials, 1997, Vol. 2.

[13]    Kazantzi AK, Righiniotis TD, Chryssanthopoulos MK. Fragility and hazard analysis of a welded steel moment resisting frame, Journal of Earthquake Engineering, 2008, Vol. 12, pp. 596-615.

[14]    Liao KW, Wen YK, Foutch DA. Evaluation of 3D steel moment frames under earthquake excitations. I: modeling, Journal of Structural Engineering, ASCE, 2007, No. 3, Vol. 133, pp. 462-470.

[15]    Chang HY, Jay Lin CC, Lin KC, Chen JY. Role of accidental torsion in seismic reliability assessment for steel buildings, Steel and Composite Structures, An International Journal, 2009, No. 5, Vol. 9, pp. 457-471.

[16]    Firat Y, Liu J. improving the dynamic response of steel structures with parameters moment frames by utilizing the lateral resistance factor of interior frames, 13th World Conference on Earthquake Engineering, Paper 285, 2004.

[17]    Reyes-Salazar A, Haldar A. Dissipation of energy in steel frames with pr connections, Structural Engineering and Mechanics, an International Journal, 2000, No. 3, Vol. 9, pp. 241-256.

[18]    Reyes-Salazar A, Haldar A. Energy dissipation at PR frames under seismic loading, Journal of Structural Engineering ASCE, 2001a, No. 5, Vol. 127, pp. 588-593.

[19]    Reyes-Salazar A, Haldar A. Seismic response and energy dissipation in partially restrained and fully restrained steel frames: an analytical study, Steel & Composite Structures, An International Journal, 2001b, No. 4, Vol. 1, pp. 459-480.

[20]    Mehrabian A, Haldar A, Reyes-Salazar A. Seismic response analysis of steel frames with post-northridge connections, steel & composite structures, An International Journal, 2005, No. 4, Vol. 5, pp. 271-287.

[21]    SAC, Structural Engineers Associated of California, Applied Technology Council and California University for Research in Earthquake Engineering, Steel Moment Frame Connections, Advisory No. 3, D-146, 1995.

[22]    Reyes-Salazar A. Ductility and ductility reduction factors for MDOF systems, Structural Engineering and Mechanics, an International Journal, 2002, No. 4, Vol. 13, pp. 369-385.

[23]    Annan CD, Youssef MA, El Naggar MH. Seismic vulnerability assessment of modular steel buildings, Journal of Earthquake Engineering, 2009, Vol. 3, pp. 1065-1088.

[24]    Haldar A, Nee KM. Elasto-plastic large deformation analysis of PR steel frames for LRFD, Computer & Structures, 1989, No. 5, Vol. 31, pp. 811-823.

[25]    Gao L, Haldar A. Nonlinear seismic response of space structures with PR connections, International Journal of Microcomputers in Civil Engineering, 1995, Vol. 10, pp. 27-37.

[26]    Reyes-Salazar A. Inelastic Seismic Response and Ductility Evaluation of Steel Frames with Fully, Partially Restrained and Composite Connections, Department of Civil Engineering and Engineering Mechanics, PhD Thesis, University of Arizona, 1997.

[27]    BOCA. 12th Edition Building Officials & Code Administration International Inc, National Building Code, 1993.